

Calibrating a 2D rockfall model using video footage to reevaluate rockfall hazard in post earthquake Christchurch

Becca Ringler¹, Louise Vick²

¹Department of Geology, Oberlin College, Oberlin, Ohio, rringler@oberlin.edu

²Department of Geological Sciences, University of Canterbury, Christchurch, New Zealand

Abstract

2-Dimensional rockfall modeling can help reshape earthquake prone areas for safe redevelopment by simulating rockfall patterns for future shaking events. Since rockfall is nearly unpredictable, 2D programs like RocFall use statistical analysis to model hypothetical run out distances, bounce heights, and velocities of falling boulders for different seismic scenarios. In this study, we looked at rockfall hazard in the Port Hills of Christchurch, New Zealand, and found that these 2D models can be effectively calibrated using video footage to compare the model with real rockfall to ensure accurate model parameters. We also deduced that even the most accurate 2D model has limited capability to model seismically induced rockfall because in only using two dimensions, it cannot fully model the dynamic process of these types of rockfall events. That being said, this calibration technique produces the most effective 2D model possible.

1. Introduction

For as long as people have been drawn to mountains, rockfall has jeopardized the safety of communities around the world. Rockfall is the process of rocks loosening from a cliff face and falling down a slope. It is a hazard of utmost concern due to the large areas of the world it affects, and because it is a nearly unpredictable event (Chen et al. 2012; Masuya et al. 2009; Stevens, 1998; Singh et al. 2013; Volkwein et al. 2011). The list of factors that can cause rockfall is extensive: geometry of slope,

29 rock type, fracturing, weathering, soil properties, freezing and thawing, water
30 infiltration, atmosphere, permeability of rock, gravity, seismicity, as well as others
31 (Volkwein et al. 2011). Seismicity is of utmost concern in Christchurch and its
32 surrounding suburbs after the 2010-2011 Canterbury Earthquake Sequence and the
33 concern for future seismic events.

34

35 Between September 2010 and June 2011, the greater Christchurch area experienced
36 the devastating Canterbury Earthquake Sequence. On September 4, 2010 the
37 Greendale fault ruptured 35 km west of Christchurch, which caused the M_w 7.1
38 Darfield earthquake. On February 22, 2011, there was a M_w 6.3 earthquake
39 approximately 10 km southeast from downtown Christchurch in the Port Hills. An
40 aftershock of this earthquake was felt on June 13, 2011 and had a M_w of 6.1, also in
41 the Port Hills. During the February Christchurch earthquake and subsequent
42 aftershocks Christchurch was heavily damaged by shaking, liquefaction, cliff
43 collapse, and rockfall. 181 people died in the Christchurch Earthquake, three from
44 cliff collapse, two from rockfall, and the rest of the fatalities were due to building
45 collapse (Bell et al., 2013).

46

47 After the Canterbury Earthquake Sequence, Christchurch began a period of
48 rebuilding that it continues today. It is a major undertaking for the city and the
49 estimated cost to rebuild is in the range of \$40 billion (Key, 2013). The shape of the
50 city has been changing in the past three years as risk assessment has deemed
51 previously populated areas of the city no longer fit to inhabit.

52

53 The Port Hills surround the city of Christchurch from the south and are comprised
54 of Miocene andesitic lava flows overlain with loess and colluvium deposits. During
55 shaking events, rocks break away from outcrops along planes of weakness, and
56 previously loosened boulders from the hill run down the slope, creating rockfall
57 hazard. The boulders are ellipsoids so they both roll and bounce down the hill in
58 irregular patterns.

59

60 Since rockfall is unpredictable, various models are used to explore all possible ways
61 this process might behave. These models provide information that informs zoning or

62 remedial decisions. In order to make realistic decisions, a well-calibrated model is
63 required that actually reflects the geology of the area and the interaction of the
64 falling boulders with the topography. Using data collected from video analysis, 2D
65 rockfall models can be created and properly calibrated to analyze this risk in similar
66 geological environments for future shaking events.

67

68 **2. Geological Setting**

69 The Port Hills are part of the extinct Lyttelton Volcanic complex, a Miocene aged,
70 basaltic volcano (Massey, 2014). The bedrock is comprised of layers of weathered
71 basalt lava flows, scoria, agglomerate, ash, and palaeosols (Massey, 2014). On top of
72 the volcanic deposits is a layer of quaternary aged loess, wind blown sand and silt,
73 which is 1 to 5 m thick (Bell and Trangmar, 1987). On top of that is talus that
74 comes from the weathered and cracked volcanic rocks that have fallen down the
75 slope (Massey et al. 2012). For this study, three slopes in the Port Hills are being
76 analyzed: Godley's Head, Boulder Bay, and Evan's Pass. The source area of the
77 rockfalls are outcrops of volcanic rock that have a slope angle greater than 37
78 degrees (Massey et al. 2012). These areas are made up of weathered lava flows and
79 scoria, which are very blocky due to irregular cooling joints (Massey, 2014).

80

81

82 **3. Methods**

83 Due to the difficulty of modeling rockfall, many different types of models exist. To
84 create our model we used the statistical analysis program RocFall, which creates a
85 2D rockfall model. This program was created to address the major difficulties of
86 rockfall analysis: variable or unknown slope materials, unknown starting location of
87 the rocks, variable slope geometry, and the fact that the calculations utilized in
88 numerical rockfall modeling were extremely sensitive to minute deviations in
89 different parameters (Stevens, 1998). To create the RocFall model and run the
90 subsequent simulations, slope, feeder zone, mass of rocks, and their velocity must be
91 known (Stevens, 1998). We acquired this information from the scaling videos.

92

93

3.1 Creating the slope

94

To get accurate slopes for all three sites and decrease user error, we used a DEM (digital elevation model) of the Port Hills, found the locations from the scaling videos, and extracted the slope using the spatial analyst tool in ArcMap. Figure 1 shows the DEM overlain with an aerial photo of the area to ensure that we identified the correct slope locations. The slope is extracted from ArcMap as X,Y coordinates in Excel. This is then entered into RocFall.

100

101

The next step is to determine the correct materials along the slope. We did this by estimating the location and extent of each material from the video footage. Each slope material has its own unique properties which affects the boulder's behavior when they make contact.

102

103

104

105

106

The main property that affects boulder trajectory is the materials Coefficient of Restitution (R). R represents the change in velocity of the boulder once it encounters the slope material, expressed as the ratio of outgoing velocity to incoming velocity (Massey et al. 2012). The value of R can be from 0 to 1. This value reflects the elasticity of the material, so a material with a high R value means that the values of incoming and outgoing velocity are very similar, which in turn means that the material is very elastic (Massey et al. 2012). An R value closer to 0 means that the material is less elastic and will slow down or stop the boulder (Massey et al. 2012). These values can be determined by either field or lab tests.

107

108

109

110

111

112

113

114

For this work, we used R values from Baishan Peng's Masters of Engineering Geology thesis at the University of Canterbury entitled "Rockfall Trajectory Analysis – Parameter Determination and Application." In this work Peng performs various experimental field and lab tests to determined coefficient of restitution for the slope materials in the Port Hills. These values are listed in Table 1.

115

116

117

118

119

120

121

3.2 Initial Seeder Conditions

122

123 Finally, a seeder area must be determined. This is the source area of the rocks in
124 the model. The initial conditions of the seeder zone were selected by reviewing
125 previous work on rockfall in the Port Hills. Rockfall can either be triggered by
126 dynamic or static initial conditions (Brehaut , 2012). Dynamic conditions refer to
127 earthquake shaking, and static conditions are any other process, such as
128 weathering, that can cause rockfall (Brehaut, 2012). In our model we used initial
129 horizontal and vertical velocity values calculated from Peak Ground Accelerations
130 during the Canterbury Earthquake Sequence (Brehaut, 2012). For boulder size we
131 selected a size similar to ones released during the February and June 2011
132 earthquakes. These values are listed under Table 2.

133

134 ***3.3 Running the model***

135 Once all of the initial parameters are entered, the user runs the model, (which
136 calculates the statistical distribution of the results). 50 boulders were released from
137 the feeder zone in each simulation. The output is a slope profile overlain with the
138 boulder trajectories, as well of graphs of the various values of runout distance,
139 bounce height, and velocity.

140

141 **3.4 Video analysis**

142 Once the simulation is run, it is necessary to analyze the video footage to see if the
143 model is behaving the same as in actuality. To do this we used Kinovea, a video
144 analysis program to extrapolate the overall trajectory pattern, bounce heights,
145 runout distances, and velocities of boulders falling down the slope. If these values
146 do not match the models, then the model is not properly calibrated and we must
147 adjust the slope properties. To determine bounce heights we used the following
148 relationship between bounce distance and height for shallow jumps [Volkwein et
149 al., 2011]:

150

$$f/s = 1/12$$

151 Velocity is calculated using an estimate for parabolic distance over time:

$$d = \left[\frac{\sqrt{s^2 + 16(f^2)}}{2} \right] + s^2 \left[\frac{\ln[4f + \sqrt{s^2 + 16(f^2)}]}{8f} \right]$$

152

$$v=d/t$$

153 f = bounce height; s = bounce distance; t = time; d = parabolic distance; v = velocity.
154 Values for bounce distance and time were taken from the video.

155

156 Once these values are determined, we compared them to the values produced in our
157 simulations. If the values were not within an acceptable range of those observed in
158 the video, then parameters were adjusted and the process of running the model and
159 comparing the results to those from the video was repeated.

160

161

162 **4. Results**

163 Results of this calibration technique are listed in the appendix. They show the
164 velocities, runout distances, and bounce heights of the calibrated model (Figures 2,
165 3, 4, 5, 6, 7, 8, 9, 10, 11) compared to those values extract from the videos (Table 3).

166

167 **5. Discussion**

168 The values calculated and observed for bounce height, velocity, and runout distance
169 in the models all are within the ranges produced by the RocFall model. This
170 indicates that using video footage is an effective way to create an accurate 2D model.
171 The action of scaling, which is captured in the videos, mirrors the dynamic motion of
172 seismically induced rockfall. Being able to watch the behavior of the rock falls in
173 the footage mirror those produced by the model assure a degree of confidence that
174 the parameters chosen for the model are correct. This process also brought to light
175 many issues with RocFall's method of 2D modeling. This, as well as limitations of
176 using video footage, are addressed below.

177

178 ***5.1 Limitations of using footage***

179 This work has shown that video footage is an extremely useful tool in creating an
180 accurate model. This technique's principal disadvantages are that this process relies
181 on the quality of the video footage. The major challenges of video footage include the
182 camera's extent, and the action of the boulders. The Boulder Bay footage was very
183 difficult to analyze because every time the boulder fell down the slope it created a

184 massive cloud of debris and dust. This obscured the boulders movements for most of
185 the initial slope, and by the time the boulder exited the dusty cloud, it was so far
186 down the slope that its movements could no longer be clearly seen or analyzed. If a
187 simple meter scale stick were placed within the video frame, this process would be
188 more precise. Although it is possible for the user to infer scale markers, there will
189 always be a certain amount of uncertainty and human error with that technique.

190

191 ***5.2 Limitations of 2D Modeling***

192 While this work has shown that 2D models can be properly calibrated, it also points
193 out many weaknesses in the technique. The accuracy of the 2D models depends
194 heavily on correct values for coefficient of restitution. Slight changes in these values
195 completely alter the rock falls trajectory because of varying material elasticity.

196 Unfortunately, coefficient of restitution is not constant throughout the slope
197 material in actuality (Peng, 2000). This means that while accurate coefficient of
198 restitution values help create a realistic model, the overall assumption of uniform
199 coefficient of resistivity through a slope material is not correct. Even if that
200 assumption were correct, coefficient of restitution is an extremely difficult value to
201 get (Peng, 2000) (Massey, 2012).

202

203 Using only two dimensions also presents limitations. RocFall and other similar
204 programs cannot predict how falling rocks will move laterally, which would impact
205 their run out distances and area. This also does not take into account for the slopes
206 the rocks may run down if they move laterally since the model only takes place on
207 one fragment of a slope. With those things in mind, perhaps a more in depth
208 modeling technique, such as 3D, should be looked into in the future for this type of
209 work.

210

211 Perhaps RocFall's greatest weakness is its treatment of the size of the falling rocks.
212 It is a hybrid model, which means it is both a lumped mass model, which considers
213 the rock to be simultaneously a weightless particle traveling down the slope, and a
214 rigid body model, which incorporates the mass of the rock. In RocFall's case, each
215 rock is represented as an immeasurably small particle in the model that are so
216 miniscule they never interact with once another (Brehaut, 2012). They have no

217 size and their mass is not used to calculate their motion as they fall, but only to
218 determine their kinetic energy (Brehaut, 2012). Their mass remains constant
219 throughout the simulation, and therefore the rocks never fragment. These
220 assumptions make the 2D model easier and quicker to use because it skims over
221 these inputs, but these assumptions are contrary to the behavior of falling rocks. In
222 all of the videos we analyzed for this calibration, the rocks fragmented as they fell
223 down the slope. For example, in the Boulder Bay footage, all of the boulders
224 released fragments as they travel down the slope. These fragments generally
225 stopped at a patch of colluvium towards the bottom of the slope, and the main
226 boulder that all of the fragments broke off of all fall into the water and the bottom of
227 the slope. In the model, every rock made it into the water. Because the model does
228 not account for the fragments, it does not have the ability to predict their runout
229 distances separate from the principle rock or consider this change in mass of the
230 principle boulder.

231

232 ***5.3 Future work***

233 Even though this technique produced a model that mirrored the reality as captured
234 in the video, it must be questioned if this simulation can really be used for
235 seismically induced rockfall. During the Canterbury Earthquake Sequence, over
236 5,000 boulders were released in the Christchurch City area (Kaiser, et al., 2012).
237 These boulders did not fall down the slope solitarily, as our boulders in the scaling
238 videos and RocFall model did. So while this calibration technique can create an
239 accurate model that is able to mirror the behavior of boulders in a scaling video, it is
240 unclear how well this process can be translated to seismically induced rockfall.

241

242 With that being said, calibrating a 2D model in this manner is probably the most
243 accurate 2D technique available at this time and the parameters we have
244 determined in this study can be used on other slopes in the Port Hills as well as
245 Bank's Peninsula for the time being. Future simulations run using these correct
246 parameters can be used to assess hazard risk in the area with a high degree of
247 confidence that the results are as accurate as possible using a 2D modeling
248 technique. The model can be run using various peak ground accelerations to

249 simulate the slope's behavior in earthquakes of various sizes. These results can be
250 combined to see what remedial techniques, if any, can be used to ensure safety.
251

252 The bounce heights, runout distance, and velocities produced by these 2D
253 simulations can help to inform engineers on the most cost effective and safe
254 remediation techniques. For example, as the rocks fall down the slope their bounce
255 height decreases. The Canterbury Earthquake Recovery Authority mandates that
256 all catchment areas be three times as tall as the maximum bounce height. By
257 modeling the bounce heights along the slope, engineers can build catchment areas
258 further down the slope that are effective, and don't need to be as tall and are
259 therefore less expensive. The same goes for velocity, and as the rocks change they
260 travel down the slope, different and more economical materials can be used to
261 construct the catchment areas.

262

263 While it is clear that 2D modeling has many limitations, it is also apparent that the
264 technique of calibrating the model using video footage increases the accuracy of
265 these models. This study is just a primary synthesis of this technique, and should
266 be further studied in the future to reiterate or refute these findings.

267

268 **6. Conclusion**

269 After the Canterbury Earthquake Sequence, the Canterbury Earthquake Recovery
270 Authority began zoning properties in the Port Hills to designate the amount of risk
271 they pose to their owners and those living around them. As of December 2013, 714
272 properties in the Port Hills have been designated as in the red zone, which means
273 that the risk to life is unacceptable (greater than 1 in 10,000) and cannot be
274 economically and logically stabilized (Canterbury Earthquake Recovery Authority,
275 2013).

276

277 In order to make the most practical zoning decisions, there needs to be an accurate
278 assessment of rockfall hazard in the area. This assessment, factored in with the
279 recurrence interval for seismic events in the greater Christchurch area, can inform

280 decisions on future land development, remediation, or abandonment. 2D models are
281 an often-used technique to assess this hazard in Christchurch. While they are easy
282 to operate, they trade off simplicity with accuracy. Using video footage to calibrate
283 these models and ensure that the parameters used are correct is a good option to
284 increase model accuracy. While future work should be done to examine the ability
285 of even the most accurate 2D model to simulate seismically induced rockfall, we
286 hope that in the time being engineers who continue to work in two dimensions will
287 adopt this technique of video calibration. Scaling work is extensively done all over
288 Christchurch and provides an untapped goldmine of footage that is extremely
289 beneficial to creating accurate models.

290
291

292 **7. Acknowledgements**

293
294 Thank you to Josh Borella for his critique and guidance, as well as the engineers at
295 Abseil Engineering for capturing and providing the video footage.

296
297

298 **References**

299

- 300 Admassu, Y. and A. Shakoor (2013), Computer simulation-based evaluation of rock fall roll-out
301 distances for catchment ditch design in Ohio, USA, *Georisk*, 7(3), 198-208.
- 302 Bell, D.H., and Trangmar, B.B., 1987. Regolith materials and erosion processes on the Port Hills,
303 Christchurch, New Zealand. Fifth International Symposium and Field Workshop on Landslides.
304 Lusanne, A.A. Balkema., 1, 77-83.
- 305 Berger, F. and L. Dorren (2005), Objective Comparison of Rockfall Models using Real Size
306 Experimental Data, *Disaster Mitigation of Debris Flows, Slope Failures and Landslides*, 345-252.
- 307 Brehaut, J. C. (2012), 2D-Modelling of Earthquake-Induced Rockfall from Basaltic Ignimbrite Cliffs at
308 Redcliffs, Christchurch, New Zealand, Master of Science in Engineering Geology, University of
309 Canterbury, .
- 310 Chen, G., L. Zheng, Y. Zhang, and J. Wu (2013), Numerical simulation in rockfall analysis: A close
311 comparison of 2-D and 3-D DDA, *Rock Mech Rock Eng*, 46(3), 527-541.

312 Cubrinovski, M., B. Bradley, L. Wotherspoon, R. Green, J. Bray, C. Wood, M. Pender, J. Allen, A.
313 Bradshaw, G. Rix, M. Taylor, K. Robinson, D. Henderson, S. Giorgini, K. Ma, A. Winkley, J. Zupan, T.
314 O'Rourke, G. DePascale, and D. Wells (2011), Geotechnical aspects of the 22 February 2011
315 Christchurch earthquake, *Bulletin of the New Zealand Society for Earthquake Engineering*, 44(4), 205-
316 226.

317 Kaiser, A. et al., 2012. The M w 6.2 Christchurch earthquake of February 2011: preliminary report.
318 *New Zealand Journal of Geology and Geophysics*, 55(1), pp.67–90.

319 Khajavi, N., M. Quigley, S. T. McColl, and A. Rezanejad (2012), Seismically induced boulder
320 displacement in the Port Hills, New Zealand during the 2010 Darfield (Canterbury) earthquake, *N. Z.*
321 *J. Geol. Geophys.*, 55(3), 271-278.

322 Koleini, M. and J. L. van Rooy (2011), Falling rock hazard index: A case study from the Marun Dam
323 and power plant, south-western Iran, *Bull. Eng. Geol. Env.*, 70(2), 279-290.

324 Massey, C., Gertenberger, M., et al., 2012. Canterbury earthquakes 2010/11 Port Hills slope stability:
325 additional assessment of the life-safety risk from rockfalls (boulder rolls) report a.

326 Massey, C.I., McSaveney, M.J., Heron, D., Lukovic, B. 2012. Canterbury Earthquakes 2010/11 Port
327 Hills Slope Stability: Pilot study for assessing life-safety risk from rockfalls (boulder rolls), GNS
328 Science Consultancy Report 2011/311.

329 Massey, C.I., McSaveney, M.J., Taig, T., Richards, L., Litchfield, N.J., Rhoades, D.A., McVerry, G.H.,
330 Lukovic, B., Heron, D.W., Ries, W., and Russ J. Van Dissen (2014) Determining Rockfall Risk in
331 Christchurch Using Rockfalls Triggered by the 2010–2011 Canterbury Earthquake Sequence.
332 *Earthquake Spectra*, 30(1), 155-181.

333 Masuya, H., K. Amanuma, Y. Nishikawa, and T. Tsuji (2009), Basic rockfall simulation with
334 consideration of vegetation and application to protection measure, *Natural Hazards and Earth System*
335 *Science*, 9(6), 1835-1843.

336 Peng, Baishan. 2000. Rockfall trajectory analysis : Parameter determination and application,
337 Master of Science in Engineering Geology, University of Canterbury, .

338 Sadagah, B. H. and S. I. El-Shanooty (2012), Modeling and remedial measures of rock slope stability
339 and rockfalls problems along Werka descent road West of Saudi Arabia, paper presented at 46th US
340 Rock Mechanics / Geomechanics Symposium 2012.

341 Singh, P. K., A. B. Wasnik, A. Kainthola, M. Sazid, and T. N. Singh (2013), The stability of road cut cliff
342 face along SH-121: A case study, *Nat. Hazards*, 68(2), 497-507.

343 Stevens, W. D. (1998), RocFall: A tool for probabilistic analysis, design of remedial measures, and
344 prediction of rockfalls, Masters of Applied Science, University of Toronto, Canada.

345 Tagliavini, F., P. Reichenbach, D. Maragna, F. Guzzetti, and A. Pasuto (2009), Comparison of 2-D and
346 3-D computer models for the M. Salta rock fall, Vajont Valley, northern Italy, GeoInformatica, 13(3),
347 323-337.

348 Vijayakumar, S., T. Yacoub, M. Ranjram, and J. H. Curran (2012), Effect of rockfall shape on normal
349 coefficient of restitution, paper presented at 46th US Rock Mechanics / Geomechanics Symposium 2012.

350 Volkwein, A., K. Schellenberg, V. Labiouse, F. Agliardi, F. Berger, F. Bourrier, L. K. A. Dorren, W.
351 Gerber, and M. Jaboyedoff (2011), Rockfall characterization and structural protection - A review,
352 Natural Hazards and Earth System Science, 11(9), 2617-2651.

353 Wang, Y., F. Tonon, and R. Guardia (2011), 2D Rock-fall simulations taking into account rock
354 fragmentation, 45th US Rock Mechanics / Geomechanics Symposium.

355

356

357

358

359

360

361

362

363

364

365

366

367

368
369

6. Appendix



370
371
372
373
374

Figure 1: DEM of the port Hills with aerial photographs superimposed showing boulder trails of the three sites.

375

	Coefficient of normal restitution (R_n)	Coefficient of tangential restitution (R_t)
Weathered basalt	0.85	--
Loess	0.17	0.35
Colluvium	0.17	0.33

376

All materials have a friction angle of 20 degrees with a standard deviation of 5.

377

Table 1: Coefficient of restitution for slope materials.

378
379

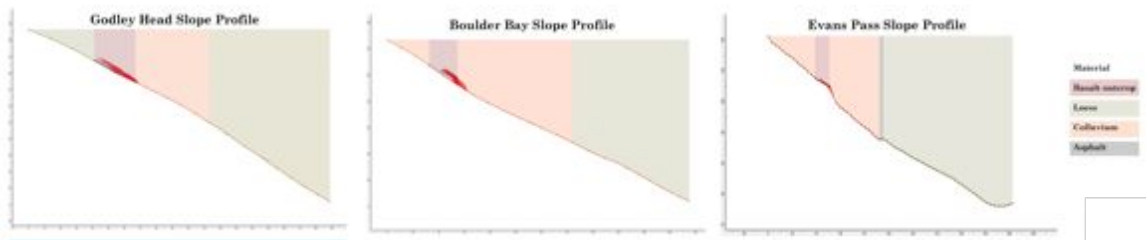
380

381

	Mean	Standard Deviation
Horizontal Velocity (m/s)	1.5	0.0
Vertical Velocity (m/s)	1.0	0.0
Mass (kg)	2700	1000
Angular Velocity	3.0	1.0

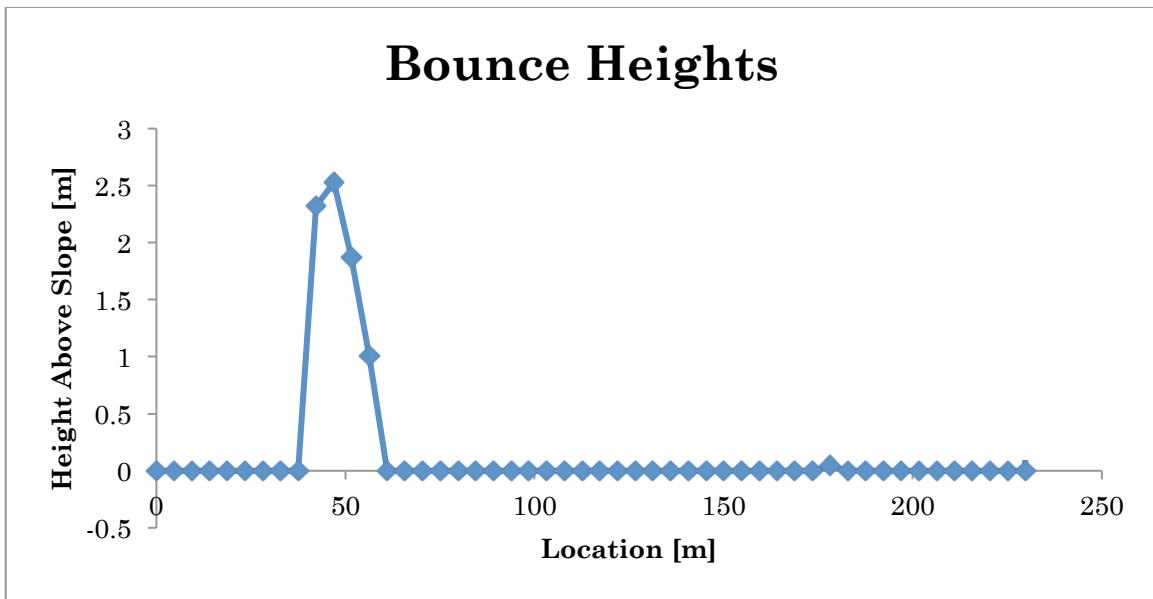
382 **Table 2: Initial seeder conditions**

383
384
385
386
387

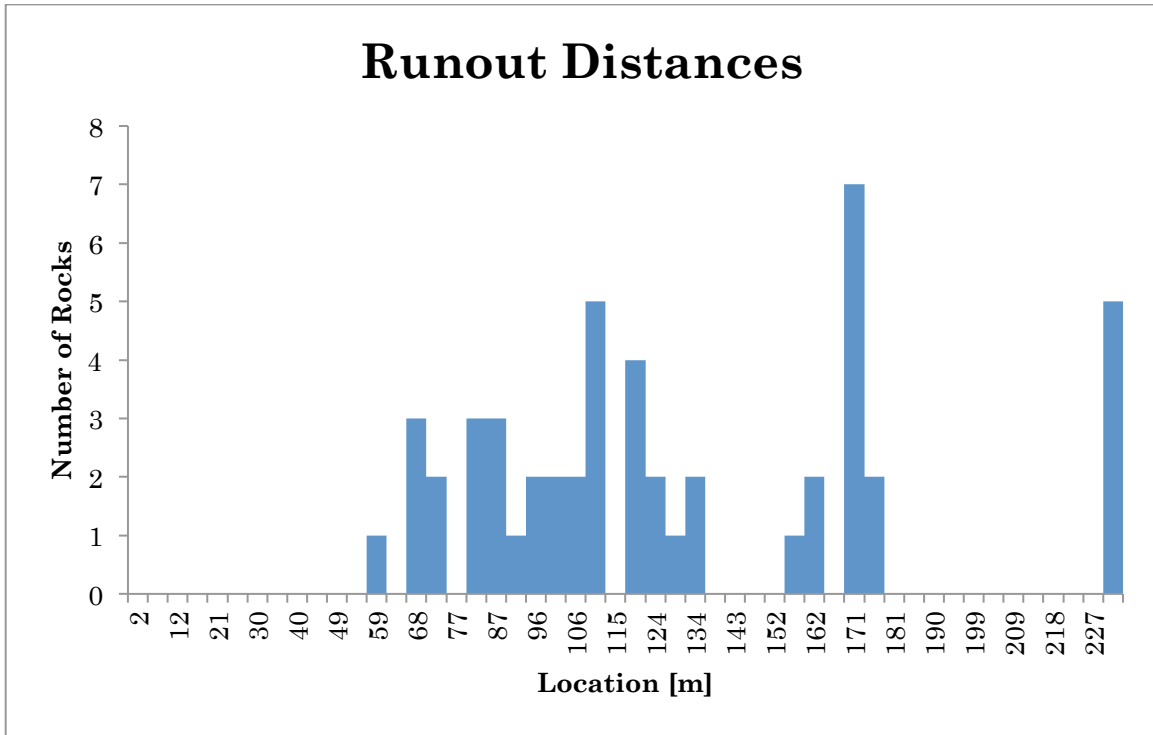


388
389 **Figure 2: RocFall produced slope profiles with boulder trajectories in red**

390
391
392
393
394

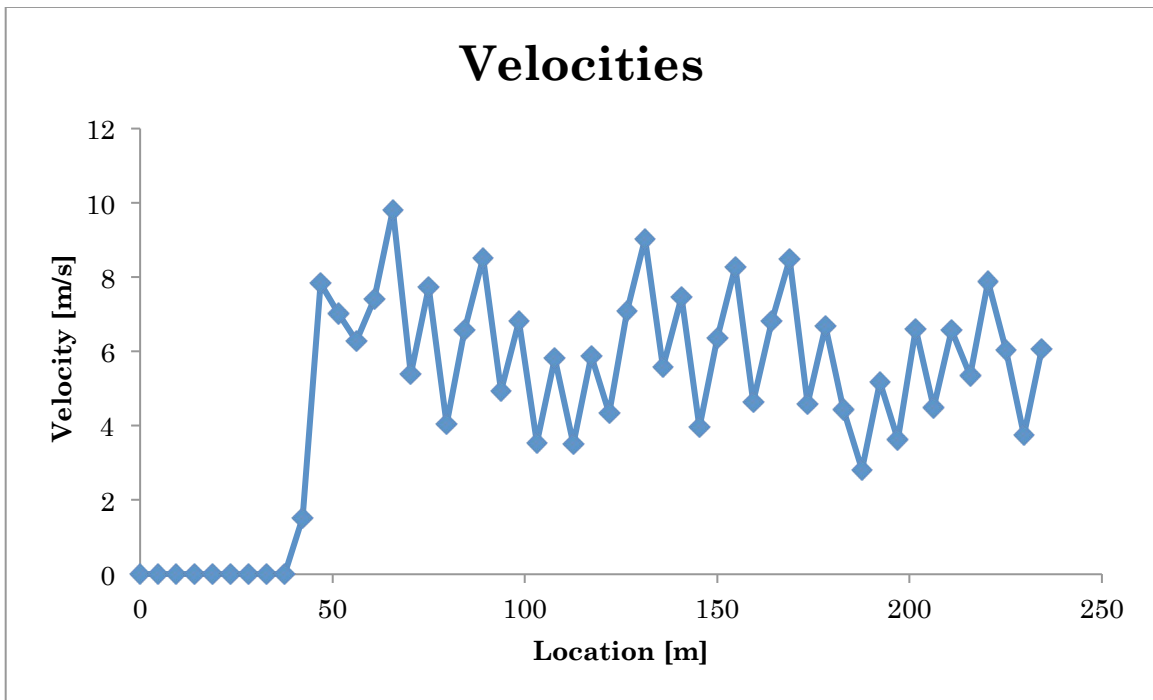


395
396 **Figure 3: Boulder Bay bounce heights**

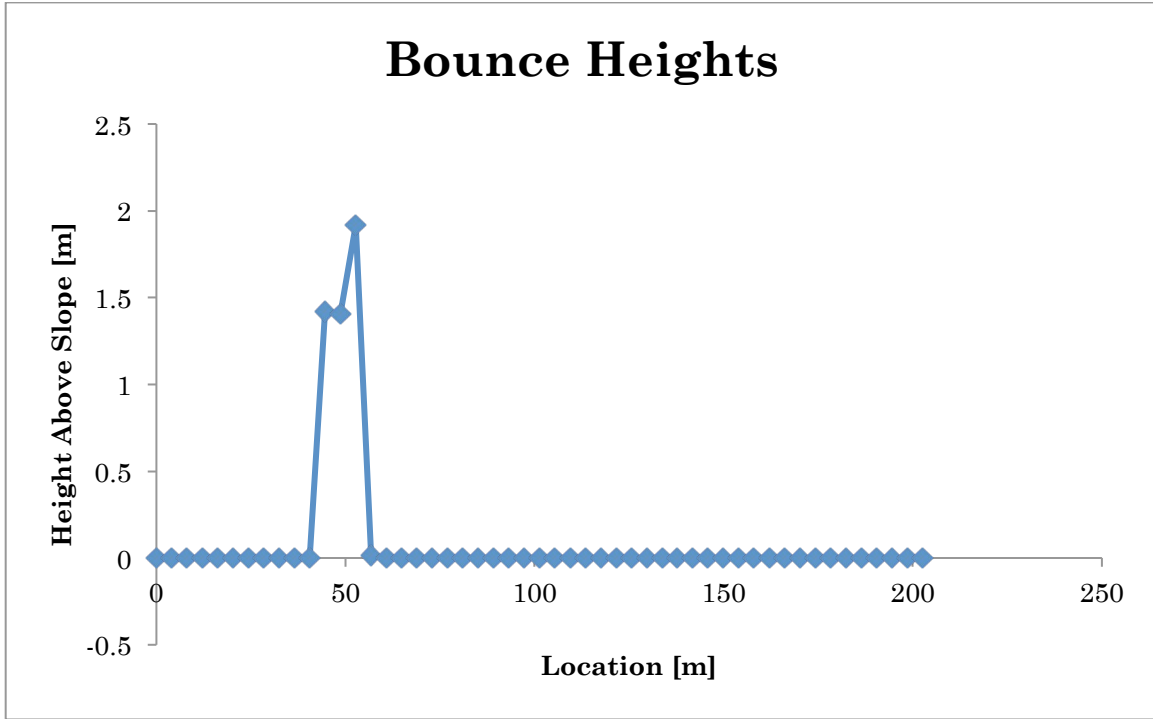


397
398 **Figure 4: Boulder Bay runout distances**

399
400
401
402
403

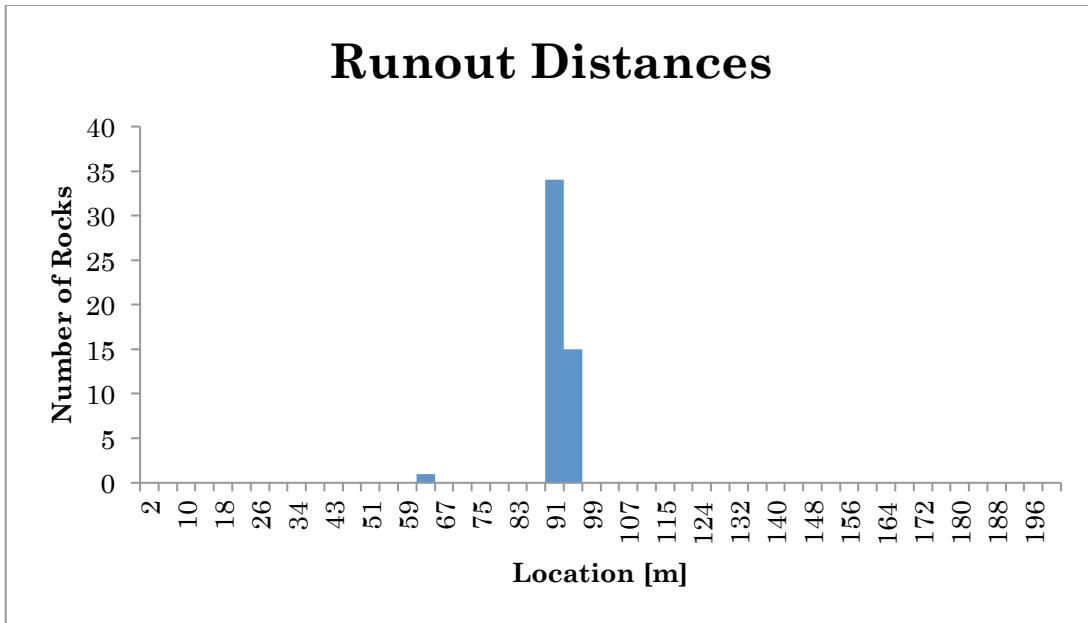


404
405 **Figure 5: Boulder Bay velocities**



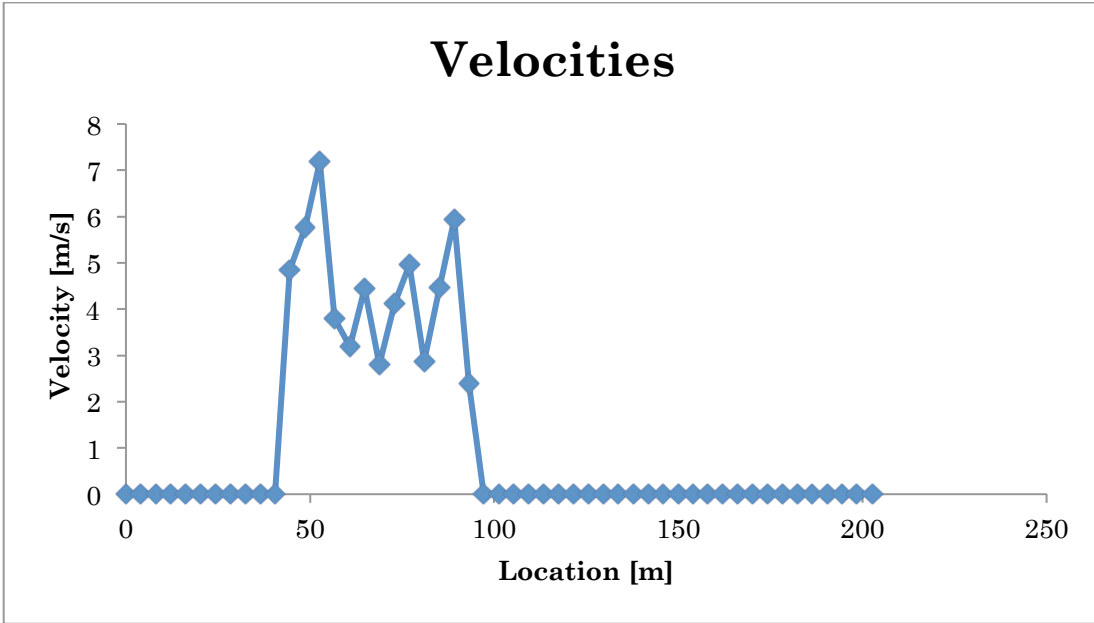
406
407
408
409
410
411
412

Figure 6: Evan's Pass bounce heights

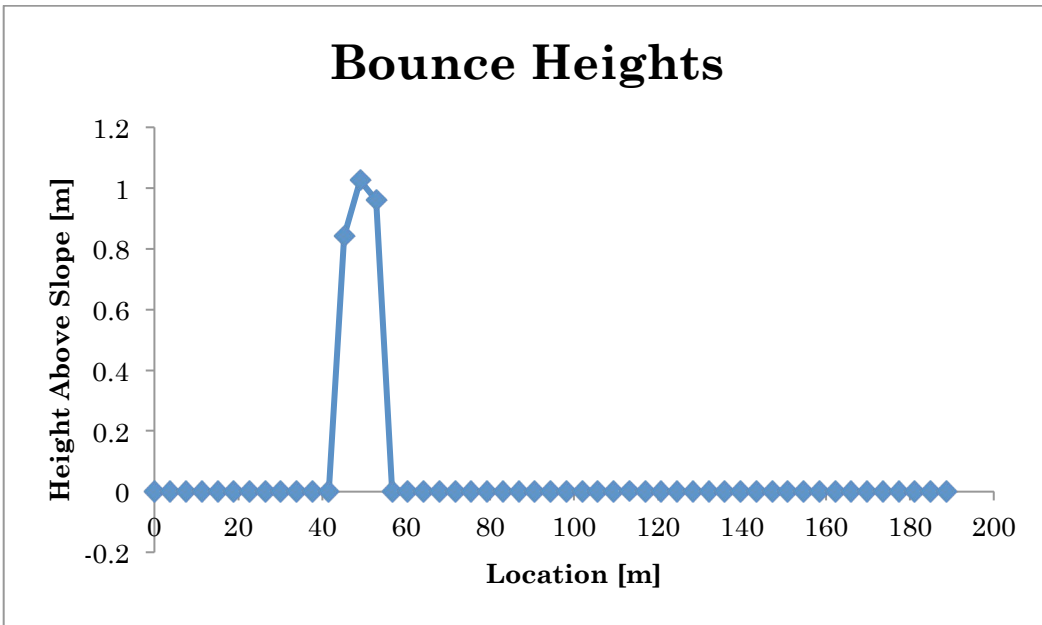


413
414

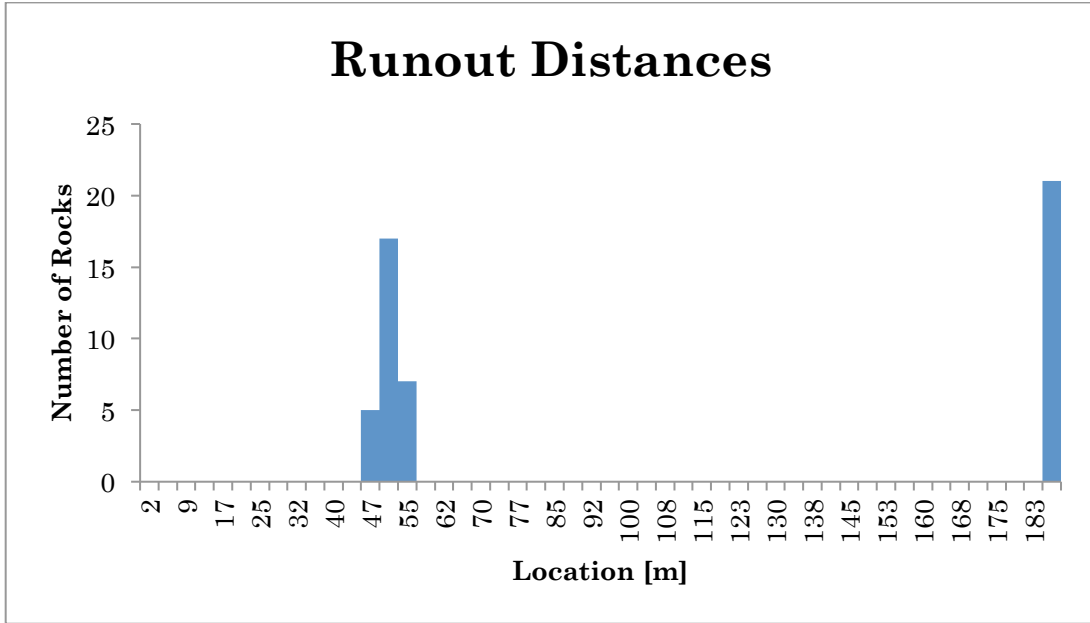
Figure 7: Evan's Pass runout distances



415
 416 **Figure 8: Evan's Pass velocities**
 417
 418
 419
 420

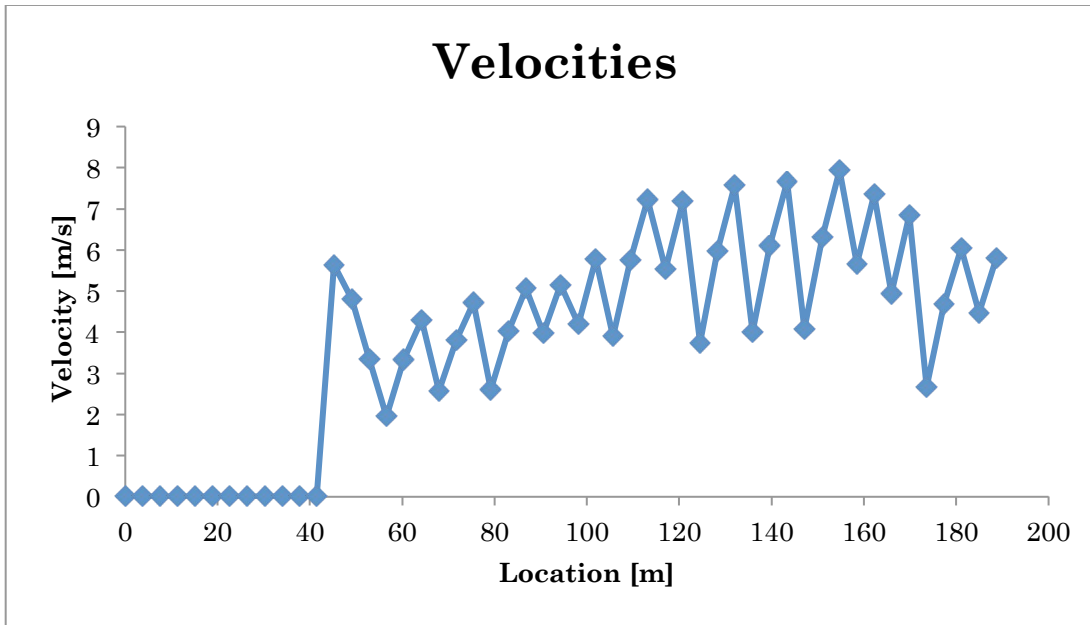


421
 422 **Figure 9: Godley's Head bounce heights**
 423
 424
 425
 426



427
428 **Figure 10: Godley's Head runout distances**

429
430
431
432
433



434
435 **Figure 11: Godley's Head velocities**

436
437
438
439
440
441

	Bounce Height (m)	Runout Distance (m)	Velocity (m/s)
Evan's Pass 1	.11	94	2.90
Evan's Pass 2	.10	96	2.77
Evan's Pass 3	.21	96	4.64
Godley Head 1	.17	190	10.20
Godley Head 2	.21	190	8.51
Godley Head 3	.27	190	8.77
Godley Head 4	.21	190	8.51
Boulder Bay	.33	--	11.66

442 **Table 3: Values of bounce height, runout distance, and velocity as**
443 **calculated from scaling video footage**